Influence of annealing temperature of ZnO film as the electron transport layer on the performance of polymer solar cells*

LI Yong-fu (李永富)[1]**, **ZHANG Ya-guang** (张亚光)[1,2], **LIU Jun-liang** (刘俊良)[1,2], and **WANG Qing-pu** (王青圃)[1]

1. Advanced Research Center for Optics, Shandong University, Jinan 250100, China

2. Institute of Crystal Materials, Shandong University, Jinan 250100, China

(Received 27 April 2015)

The surface morphology of ZnO films at different annealing temperatures and the performance of polymer solar cells (PSCs) with ZnO as the electron transport layer are studied. The low temperature sol-gel processed ZnO film has smoother surface than that in higher temperature, which results in the best photovoltaic performance with a power conversion efficiency (*PCE*) of 3.66% for P3HT:$PC_{61}BM$ based solar cell. With increasing annealing temperature, the photovoltaic performance first deceases and then increases. It could be ascribed to the synergy effects of interface area, the conductivity and surface energy of ZnO film and series resistance of devices.

Document code: A **Article ID:** 1673-1905(2015)04-0260-4

DOI 10.1007/s11801-015-5072-4

Polymer solar cells (PSCs) based on blends of conjugated polymers and fullerene derivatives have attracted great attention because of light weight and potentially low cost from printing at low temperature on flexible substrates[1-5].

In order to solve the problems about PSCs, inverted PSCs have been developed, where a high-work-function metal (e.g., Ag) serves as the anode and indium tin oxide (ITO) coated glass serves as the cathode. However, ITO cannot serve as cathode directly. It requires interfacial modification with functional electron transport layers (ETLs) for hole blocking and electron extraction. The n-type metal oxides, such as zinc oxide (ZnO)[6-11] and titanium oxide (TiO_x)[12,13], deposited onto the ITO electrode are good choice to break the symmetry. Among the n-type metal oxide ETLs, ZnO is one of the most intensely studied materials for this function due to its high electron mobility and high degree of transparency in the visible wavelength range[14-16]. Moreover, ZnO is an ideal ETL for wide band gap and good positioning of the conduction band of ZnO (−4.4 eV) in combination with [6,6]-phenyl C61 butyric acid methyl ester ($PC_{61}BM$). There have been many methods to construct ZnO layer for efficient inverted PSCs, such as sputtering[8], sol-gel process[9,10] and hydrothermal[11]. The sol-gel process has distinct potential advantages due to its lower crystallization temperature, ability to tune microstructure, compositional control and large surface area coating capability. The preparation of ZnO films by the sol-gel process for PSCs has already been reported. However, there is no report about the influence of preparing temperature of sol-gel processed ZnO layer on the performance of PSCs.

In this paper, the ZnO films were coated on ITO coated glass substrates by a cheap and modified sol-gel method at different post annealing temperatures. The optical and morphological properties of the films were examined and characterized. Then the films were fabricated into PSCs as ETL. The influence of ZnO film annealing temperature on the performance of inverted PSCs is explored systemically. The results show that the size of ZnO particles and the surface roughness of films are gradually increased when increasing annealing temperature. The photovoltaic performance firstly decreases and then increases. The best power conversion efficiency (*PCE*) of poly(3-hexylthiophene) (P3HT) and $PC_{61}BM$ based solar cell is 3.66% with ZnO layer annealed at 100 °C for 17 h.

For preparing the ZnO film, the zinc acetate dihydrate ($Zn(CH_3COO)_2{\cdot}2H_2O$, AR grade) and monoethanolamine (MEA, AR grade) were dissolved in 2-ethoxyethanol, and the zinc concentration was 0.5 mol/L. The mixture was stirred to obtain a clear homogeneous ZnO precursor solution for further use. The ITO-coated glasses were cleaned in an ultrasonic bath with acetone, ITO detergent, ultra pure water and isopropyl alcohol for 20 min. The ZnO precursor solution was spin coated at 4 000 r/min

* This work has been supported by the Independent Innovation Foundation of Shandong University (No.2014YQ015).

** E-mail: yfli@sdu.edu.cn

for 40 s on the ITO coated glass substrate. The films were first annealed at 100 °C for 16 h in an oven, and then treated at 100 °C, 200 °C, 300 °C, 400 °C and 500 °C for another 1 h, respectively, and the films and their PSCs were named as A1–A5, respectively.

The substrates were transferred into glove-box after the preparation of ZnO films. Subsequently, a blend solution of P3HT (Lumtec Inc.) and $PC_{61}BM$ (American Dye Sources Inc.) with a weight ratio of 1:1 in chlorobenzene (CB) was spin coated to form the active layers (120 nm), and then the active layer was annealed on a hotplate at 150 °C for 10 min. Next, molybdenum oxide (MoO_3, 5 nm) and silver (Ag, 80 nm) were thermally evaporated under 2.0×10^{-4} Pa. Finally, the solar cells with an active area of 0.1 cm^2 defined by shadow mask were prepared.

The current density-voltage (*J-V*) characteristics were measured with a Keithley 2400 source measurement unit under simulated 100 mW/cm^2 (AM 1.5 G) irradiation. The light intensity was calibrated with a standard silicon solar cell. The thickness of the active layer was determined by Dektak 150 profilometer. The surface morphologies of ZnO films and active layers were investigated by atomic force microscopy (AFM) in tapping mode. The active layers for AFM measurement were obtained by spin coating P3HT:$PC_{61}BM$ solution on top of ITO coated glass substrates covered with ZnO films under different treatment conditions. The wettability of the films was characterized with an automated contact goniometer.

ZnO has high electron mobility which makes it an ideal ETL in PSCs. The quality of ZnO layer is an important factor in the optimization of the performance of the PSCs. The annealing effect of ZnO films is investigated, and three representative AFM images of samples A1, A3 and A5 are shown in Fig.1(a), (c) and (e). The results show that ZnO films are smooth and composed of nanoparticles with diameters around 9 nm for A1 sample. The size of particles and the surface roughness of the films both gradually increase when further annealing under increasing temperature, such as A3 and A5 shown in Fig.1(c) and (e). When the annealing temperature changes from 100 °C to 500 °C, the grain size of ZnO nanoparticles varies from about 9 nm to 50 nm, and the root-mean-square (*RMS*) roughness becomes larger from 1.76 nm to 2.16 nm. The nanoparticles of ZnO cluster together, forming larger grains, which results in a little rougher surface morphology of the films under higher annealing temperature. The AFM images suggest that the ZnO film annealed at 100 °C has the smallest effective surface area, and thus has the smallest effective interfacial area between the ZnO layer and the active layer on top, whereas the ZnO film annealed at 500 °C has the largest effective interfacial area with the active layer.

To investigate the influence of annealing conditions of ZnO layer on the photovoltaic performance of the PSCs, the photoactive layer was fabricated by spin coating a solution of P3HT:$PC_{61}BM$ (1:1 by weight) in CB. The topographic images of the active layers deposited on top of different ZnO layers shown in Fig.1(a), (c) and (e) taken with tapping-mode are given in Fig.1(b), (d) and (f), respectively. The AFM images show that the active layer on top of the smoother ZnO film has the finest structure, and the roughness of P3HT:$PC_{61}BM$ active layer changes a little on these three ZnO layers with different annealing conditions.

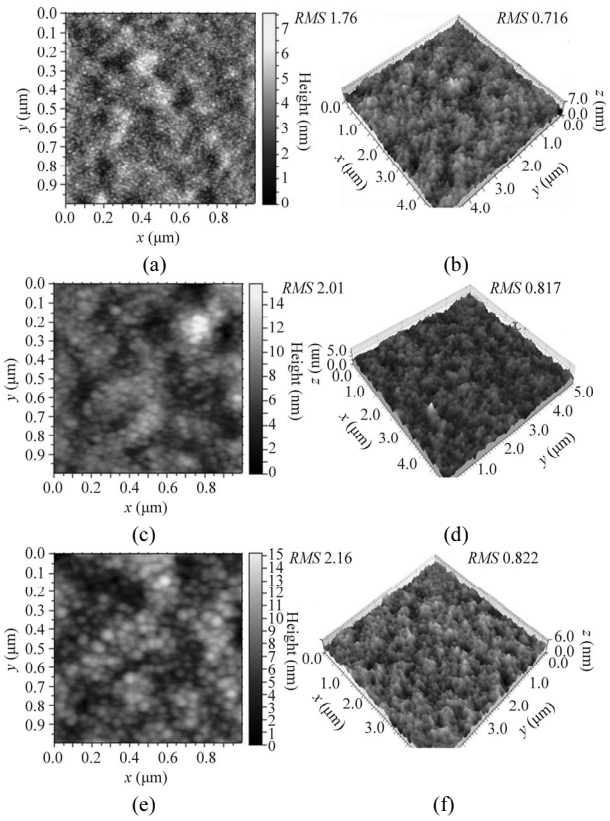

Fig.1 AFM images (1 μm×1 μm) of ZnO films at different annealing temperatures: (a) 100 °C (*RMS*=1.76 nm), (c) 300 °C (*RMS*=2.01 nm) and (e) 500 °C (*RMS*=2.16 nm); (b), (d), (f) Corresponding topographic images of active layer on the ZnO films to (a), (c), (e), respectively

The corresponding current density versus voltage (*J-V*) characteristics of five devices based on different ZnO films are shown in Fig.2. Their photovoltaic parameters are summarized in Tab.1 and plotted in Fig.3. The results show that the best performance of PSC with a *PCE* of 3.66%, a short current density (J_{SC}) of 8.52 mA/cm^2, an open circuit voltage (V_{OC}) of 0.643 V and a fill factor (*FF*) of 0.671 is based on ZnO ETL annealed at 100 °C for 17 h. When the annealing temperature of additional 1 h increases to 200–500 °C, *PCE*, J_{SC}, V_{OC} and *FF* of the PSCs all firstly decrease and then increase as shown in Fig.3. When the annealing temperature increases to 400 °C, *PCE* decreases to 2.22%, *FF* changes to 0.501, and J_{SC} and V_{OC} reduce to 7.87 mA/cm^2 and 0.563 V, respectively. Interestingly, the above four parameters all increase when the annealing temperature increases to 500 °C. As discussed in Fig.1, the *RMS* roughness in-

creases with the increase of annealing temperature. The effective interfacial area between the ZnO layer and the active layer depends on the ZnO surface roughness. According to Ref.[17], the larger the ZnO/active layer interfacial area, the more the interface traps. The interface traps, leading to an undesired trap-assisted recombination, can reduce *FF* and J_{SC} of the PSC, and thus increase the *PCE*. As can be seen in Tab.1, the series resistance (R_S) value decreases and the sheet resistance (R_{SH}) increases gradually with higher temperature, which also gives rise to poor *FF* and J_{SC}. Moreover, the resistance of ITO film (R_{ITO}) increases with the increase of annealing temperature, which could be another reason for the reduced photovoltaic performance. However, when the annealing temperature increases to 500 °C, the values of *PCE*, J_{SC} and *FF* unexpectedly have a rebounding change. It is supposed that the possible reason for enhanced performance of device at annealing temperature of 500 °C is the improved crystallinity of ZnO film and the promoted charge transport[18], but the A5 device still has very low photovoltaic performance.

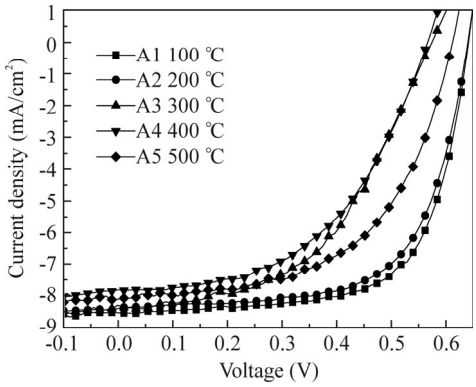

Fig.2 *J-V* curves of devices with different ZnO film annealing temperatures under AM 1.5G light illumination at 100 mW/cm²

Tab.1 The resistances of ITO, diameters of ZnO nanoparticles and photovoltaic parameters for all PSCs

Device	ZnO film treated condition	V_{OC} (V)	J_{SC} (mA/cm²)	*FF* (%)	*PCE* (%)	R_S (Ω·cm²)	R_{SH} (Ω·cm²)	R_{ITO} (Ω)	D_{ZnO} (nm)
A1	100 °C , 17 h	0.639	8.52	67.1	3.66	8.1	1 037.7	25	9
A2	100 °C , 16 h; 200 °C , 1 h	0.643	8.40	65.2	3.49	9.0	1 086.8	30	/
A3	100 °C , 16 h; 300 °C , 1 h	0.571	8.39	50.1	2.41	28.0	623.6	33	35
A4	100 °C , 16 h; 400 °C , 1 h	0.563	7.87	50.1	2.22	19.6	768.1	80	/
A5	100 °C , 16 h; 500 °C , 1 h	0.609	8.07	55.6	2.75	12.8	816.7	110	50

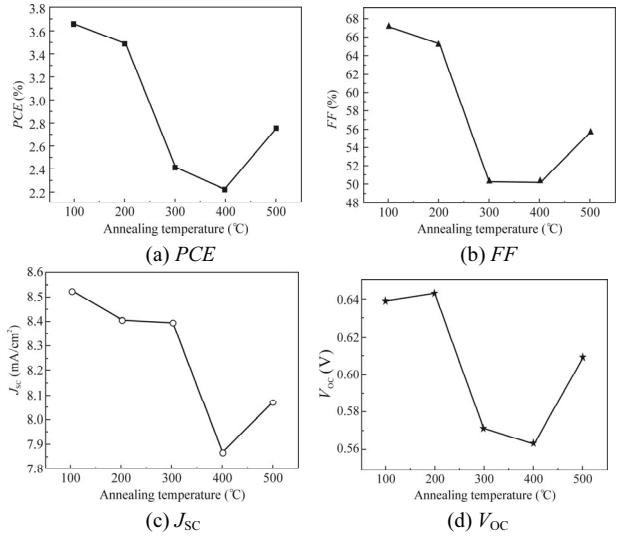

(a) *PCE* (b) *FF* (c) J_{SC} (d) V_{OC}

Fig.3 Photovoltaic parameters of the PSCs with ZnO film as ETL at different annealing temperatures

The surface energy of the substrate is reported to affect the morphology of the film deposited at top[19,20]. The morphology and the surface roughness of the ZnO layer contribute to the surface energy and influence the interfacial property of the ZnO layer/active layer, so the photovoltaic performance of the PSCs is expected to be dependent on the ZnO surface roughness. We also investigate the surface energy of the ZnO layers through water contact angle measurement. As shown in Fig.4, the water contact angle decreases from 75.88° to 64.55° for the ZnO film when the annealing temperature increases from 100 °C to 500 °C. With higher annealing temperature, the ZnO films have an increasing hydrophobicity, which agrees with the reported study that the contact angle decreases with surface roughness for hydrophilic surface. Generally, the small contact angle indicates hydrophilic property, good wetting and adhesion. Based on the contact angle measurement, we can conclude that ZnO films of devices at different conditions have variable wettability and adhesion to the polymer blend layer, and hence the performances of devices are different. The bigger water contact angle results in smoother ZnO film, and the morphologies and D/A interfacial area in the active layers on top of the different ZnO layers should be better. It is possible that the improvement in the device performance is related to better surface quality of the film, which provides better wettability and adhesion with photoactive layer.

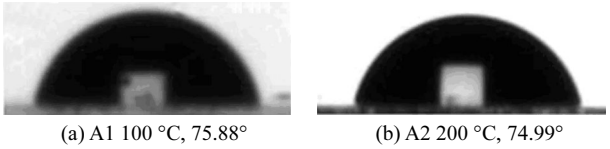

(a) A1 100 °C, 75.88° (b) A2 200 °C, 74.99°

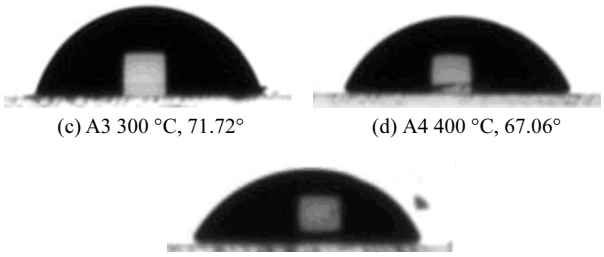

(c) A3 300 °C, 71.72° (d) A4 400 °C, 67.06°

(e) A5 500 °C, 64.55°

Fig.4 Measured water contact angles between a drop of deionized water and the ZnO films with different annealing temperatures

In summary, we systematically investigate the effects of annealing temperature of ZnO film on the performance of the inverted PSCs. The low temperature sol-gel processed ZnO film has smoother surface than that at higher temperature, which has smaller interface area and fewer interface traps. The best photovoltaic performance with *PCE* of 3.66% is obtained for P3HT:PC_{61}BM based solar cell with ZnO ETL annealed at 100 °C for 17 h. With increasing annealing temperature, the photovoltaic performance first deceases and then increases. The reason is the synergy effect of interface area, conductivity and surface energy of ZnO film and series resistance of devices. The surface morphology and appropriate annealing temperature of ZnO layer are quite important to the performance of PSCs.

References

[1] S. Gunes, H. Neugebauer and N. S. Sariciftci, Chemical Reviews **107**, 1324 (2007).

[2] Y. Zhou, J. Pei, Q. Dong, X. Sun, Y. Liu and W. Tian, The Journal of Physical Chemistry C **113**, 7882 (2009).

[3] Y. Liang, Z. Xu, J. Xia, S.-T. Tsai, Y. Wu, G. Li, C. Ray and L. Yu, Advances Materials **22**, E135 (2010).

[4] B. Yin, L. Yang, Y. Liu, Y. Chen, Q. Qi, F. Zhang and S. Yin, Applied Physics Letters **97**, 023303 (2010).

[5] L. Dou, J. You, J. Yang, C.-C. Chen, Y. He, S. Murase, T. Moriarty, K. Emery, G. Li and Y. Yang, Nature Photonics **6**, 180 (2012).

[6] XU Xin-rui, QIN Wen-jing, DING Guo-jing, LIU Dong-yue, MA Chun-yu and YIN Shou-gen, Journal of Optoelectronics·Laser **24**, 2295 (2013). (in Chinese)

[7] LIU Dong-yue, QIN Wen-jing, DONG Ni, ZHANG Qiang, YANG Li-ying and YIN Shou-gen, Journal of Optoelectronics·Laser **25**, 1363 (2014). (in Chinese)

[8] H. Cheun, C. Fuentes-Hernandez, Y. Zhou, W. J. Potscavage Jr., S. J. Kim, J. Shim, A. Dindar and B. Kippelen, The Journal of Physical Chemistry C **114**, 20713 (2010).

[9] A. K. K. Kyaw, X. W. Sun, C. Y. Jiang, G. Q. Lo, D. W. Zhao and D. L. Kwong, Applied Physics Letters **93**, 221107 (2008).

[10] X. Bao, A. Yang, Y. Yang, T. Wang, L. Sun, N. Wang and L. Han, Physica B: Condensed Matter **432**, 1 (2014).

[11] A. Apostoluk, Y. Zhu, B. Masenelli, J.-J. Delaunay, M. Sibiński, K. Znajdek, A. Focsa and I. Kaliszewskac, Microelectronic Engineering **127**, 51 (2014).

[12] Z. Lin, C. Jiang, C. Zhu and J. Zhang, ACS Applied Materials & Interfaces **5**, 713 (2013).

[13] X. Bao, L. Sun, W. Shen, C. Yang, W. Chen and R. Yang, Journal of Materials Chemistry A **2**, 1732 (2014).

[14] D. C. Look, Materials Science and Engineering: B **80**, 383 (2001).

[15] Ü. Özgur, Y. Alivov, C. Liu, A. Teke, M. A. Reshchikov, S. Doğan, V. Avrutin, S.-J. Cho and H. Morkoç, Journal of Applied Physics **98**, 041301 (2005).

[16] X. Bao, Y. Yang, A. Yang, N. Wang, T. Wang, Z. Du, C. Yang, S. Wen and R. Yang, Materials Science and Engineering: B **178**, 263 (2013).

[17] Z. Ma, Z. Tang, E. Wang, M. Andersson, O. Inganas and F. Zhang, The Journal of Physical Chemistry C **116**, 24462 (2012).

[18] Y. Natsume and H. Sakata, Thin Solid Films **372**, 30 (2000).

[19] Z. Tang, L. M. Andersson, Z. George, K. Vandewal, K. Tvingstedt, P. Heriksson, R. Kroon, M. R. Andersson and O. Inganäs, Advanced Materials **24**, 554 (2012).

[20] X. Bulliard, S.-G. Ihn, S. Yun, Y. Kim, D. Choi, J.-Y. Choi, M. Kim, M. Sim, J. H. Park, W. Choi and K. Cho, Advanced Functional Materials **20**, 4381 (2010).